5 October 1998

PHYSICS LETTERS A

ELSEVIER

Physics Letters A 247 (1998) 75–86

On the semiclassical limit of the focusing nonlinear Schrödinger equation

Peter D. Miller [1], Spyridon Kamvissis [2]

School of Mathematics, Institute for Advanced Study, Princeton, NJ 08540, USA

Received 12 May 1998; revised manuscript received 13 July 1998; accepted for publication 13 July 1998
Communicated by C.R. Doering

Abstract

We present numerical experiments that provide new strong evidence of the existence of the semiclassical limit for the focusing nonlinear Schrödinger equation in one space dimension. Our experiments also address the spatiotemporal structure of the limit. Like in the defocusing case, the semiclassical limit appears to be characterized by sharply delimited regions of space-time containing multiphase wave microstructure. Unlike in the defocusing case, the macroscopic dynamics seem to be governed by elliptic partial differential equations. These equations can be integrated for analytic initial data, and in this connection, we interpret the caustics separating the regions of smoothly modulated microstructure as the boundaries of domains of analyticity of the solutions of the macroscopic model. For more general initial data in common function spaces, the initial value problem is ill-posed. Thus the semiclassical limit of a sequence of well-posed initial value problems is an ill-posed initial value problem. © 1998 Published by Elsevier Science B.V.

PACS: 02.30.Jr; 03.40.Kf; 03.50.Kk; 03.65.Sq
Keywords: Semiclassical limits; Nonlinear Schrödinger equations; Integrable systems; Nonequilibrium thermodynamics

1. Introduction

This Letter is concerned with the behavior of solutions of the initial value problem for the focusing nonlinear Schrödinger (NLS) equation

$$\mathrm{i}\hbar\partial_t\psi + \frac{\hbar^2}{2}\partial_x^2\psi + |\psi|^2\psi = 0\,, \qquad \psi(x,0) = A(x)\exp[\mathrm{i}S(x)/\hbar]\,, \tag{1}$$

in the semiclassical limit of $\hbar \downarrow 0$. We consider $A(x)$ and $S(x)$ to be real and smooth and $A(x)$ to be positive and rapidly decreasing in $|x|$ while $S(x)$ takes on constant values $S_\pm$ as $x \to \pm\infty$. The data $A(x)$ and $S(x)$

[1] Contact address: Department of Mathematics and Statistics, Monash University, Clayton, Victoria 3168, Australia. E-mail: millerpd@neumann.maths.monash.edu.au. Supported at IAS by NSF grant DMS 9304580.
[2] Contact address: Department of Mathematics and CNRS Unit 6632 (LATP), University of Aix–Marseilles, France. E-mail: spyros@gauss.math.jussieu.fr.

PII S0375-9601(98)00565-9

do not depend on $\hbar$. The semiclassical scaling of the NLS equation occurs naturally in nonlinear fiber optics (see, e.g., Ref. [1] for a discussion of this point; of course in this application the small parameter $\hbar$ is not interpreted as a dimensionless form of Planck's constant, but rather as a ratio of optical wavelength to some fixed macroscopic scale). The defocusing version of (1), where $|\psi|^2$ is replaced by $1 - |\psi|^2$, was proposed by Ginzburg and Pitaevskii [2] as a fundamental field theoretic model of superfluidity. Here, the semiclassical limit describes a hydrodynamical state that is a mixture of a smooth superfluid background where the "order parameter" $|\psi(x,t)|^2 \sim 1$ surrounding pockets of (vortex-dominated in two or more space dimensions) normal fluid where $|\psi(x,t)|^2 \sim 0$; it is thus a model for the nonequilibrium thermodynamics of a mixture of material phases. On the other hand, the semiclassical limit of (1) is of considerable mathematical interest in its own right because it provides an example of a problem which can be solved exactly for each fixed value of $\hbar$ [3], but for which a complete understanding of the semiclassical limit is still missing. We have recently performed some numerical experiments that indicate with great confidence that the semiclassical limit exists at least for analytic initial data, and we shall describe these experiments and their results below.

2. Phenomenology of the focusing semiclassical limit

The semiclassical initial value problem (1) is a notoriously difficult one to study numerically. It is a classic example of a "stiff" problem, as it contains two different spatial and temporal scales. Ignoring the initial data for the moment, we see that the problem (1) has families of solutions that have the form $\psi = \Psi(x/\hbar, t/\hbar)$, where Ψ is some function with no explicit dependence on $\hbar$. In a sense, Eq. (1) "wants" to form *microstructure* described at least locally by functions of this form.

But there is also the fixed length scale of the initial data $A(x)$ and $S(x)$ to consider. The initial presence of this fixed scale prevents the semiclassical limit from being made up of uniform microstructure alone. Thus, there is also *macrostructure*, that is, dependence in the solution on the unscaled variables x and t. The semiclassical limit is complicated and interesting because it involves essential competition between effects on two vastly different scales. One would like to know, for example, what kind of microstructure one should expect to see in the neighborhood of fixed values of x and t.

Without a rigorous analytical theory (see below), it is natural these days to study the problem (1) numerically, say using a Fourier split-step method. The stiffness of the problem makes this difficult. Resolving the microstructure accurately requires one to use a time step that scales like $\hbar$, and then to resolve the macrostructure requires one to take a number of time steps that scales like $\hbar^{-1}$. This is a situation that quickly leads to large global errors as the local errors due to truncation and roundoff accumulate. An additional practical consideration is the number of gridpoints (or Fourier modes) required to resolve the spatial microstructure; since one needs $O(\hbar^{-1})$ of them, simulations require much memory and time. However, even if one can find a machine that is fast and big enough, one must still contend with the influence of accumulated roundoff errors on the macrostructure.

The numerical studies that have been carried out and published [4,5] may be difficult to interpret precisely, but they do indicate some important and perhaps universal features of the limiting solutions. Initially smooth "single-hump" fields focus, the primary mechanism being the Benjamin–Feir modulational instability. After the first focus event the field consists of an expanding oscillatory central region and quiescent tails on either side. It appears that the (moving) boundary between the quiescent region and the oscillatory region is very sharp for small $\hbar$; we shall call this the *primary caustic*. The oscillations that form beyond the focus are spatiotemporally complex. They certainly are not the simple traveling waves that one sees after the first breakdown in the defocusing version of the semiclassical limit [4–6]. It has been suggested that the semiclassical limit might consist of chaotic microstructure in this oscillatory region. Unfortunately, most of the published numerical experiments are carried out only for a single (small) value of $\hbar$, so it is not possible to make any definitive scaling observations that isolate the microstructure from the macrostructure.

It is clear that the limit, if it exists in any sense at all, cannot be a strong limit of the field $\psi(x,t)$. In particular, if the phase $S(x)$ is nonzero, then even the initial data does not converge strongly, and the weak limit is zero. What one might expect to converge (although perhaps weakly) are the conserved local densities of (1), like the field density $\rho(x,t)$ and the momentum $\mu(x,t)$ defined by

$$\rho = |\psi|^2 , \qquad \mu = \hbar \operatorname{Im} \overline{\psi} \partial_x \psi . \tag{2}$$

It is an old observation that semiclassical Schrödinger equations can be viewed as singular perturbations of compressible Euler-type fluid dynamical systems in the density and momentum variables. For example, the focusing nonlinear problem (1) can be written as

$$\partial_t \rho + \partial_x \mu = 0 , \qquad \partial_t \mu + \partial_x \left(\frac{\mu^2}{\rho} - \frac{\rho^2}{2} \right) = \frac{\hbar^2}{4} \partial_x (\rho \partial_x^2 \log \rho) , \tag{3}$$

with initial data $\rho(x,0) = A(x)^2$ and $\mu(x,0) = A(x)^2 S'(x)$. One would like to argue that, at least for small t, the truncated system (Euler system) obtained by dropping the term involving $\hbar$ is satisfied by the limiting density $\rho(x,t)$ and momentum $\mu(x,t)$. Self-consistency is essential for this argument, and the difficulty here is that the Euler system is elliptic. It follows that the initial value problem for the Euler system corresponding to (1) is ill-posed. From the point of view of compressible fluid mechanics, this Euler system describes a strange fluid whose pressure decreases when the density increases. As nonsensical as it may seem at the moment, we will see good evidence below that this elliptic Euler system indeed governs the initial phase of the semiclassical limit, at least for some data.

In fact, ill-posed initial problems often occur in the idealized modeling of unstable physical processes. For example, in the mechanics of incompressible inviscid fluids, two-dimensional flows are often irrotational except in the immediate neighborhood of a (moving) curve that is ideally modeled as a *vortex sheet*. The motion of a vortex sheet is described by the Birkhoff–Rott singular integro-differential equation; the initial value problem for this equation is ill-posed [7]. If the vorticity distribution is smooth, the initial value problem for the velocity field is locally well-posed, but ill-posedness appears in the limit when the initial vorticity becomes concentrated on the vortex sheet. There is a kind of dictionary of correspondences between the ill-posed dynamics of vortex sheets and the semiclassical dynamics of the focusing NLS problem (1). In both cases, the ill-posedness arises as a result of studying the limit of a sequence of well-posed problems that exhibit finite growth rate instabilities. In fluid mechanics, the physical mechanism leading to ill-posedness is the Kelvin–Helmholtz instability, whose maximum growth rate grows with gradients of the initial vorticity distribution; in the semiclassical problem (1) it is the Benjamin–Feir or modulational instability whose maximum growth rate increases as $\hbar$ decreases to zero leading to ill-posedness in the limit. In both problems the analyticity of initial data, admittedly a mathematical abstraction, appears to encode important physical information about sensitivity to instabilities.

The Euler system is meant to describe the macroscopic dynamics of solutions to (1) when the microstructure is locally a plane wave. Forest and Lee [8] have given the construction of "multiphase" wavetrain solutions of the focusing NLS equation having the form

$$\psi(x,t) = A(S_1(x,t)/\hbar, \ldots, S_g(x,t)/\hbar) \exp[\mathrm{i} S_0(x,t)/\hbar] , \tag{4}$$

where A is 2π-periodic in each argument and the $S_k(x,t)$ are linear functions of x and t. The number g is the genus of an associated Riemann surface Γ. When $g = 0$, these are the plane waves for which ρ and μ are constants (there is the additional phase constant $S_0(0,0)$). Generally, these solutions are parametrized by $2g+2$ "action" constants λ_k corresponding to the moduli of Γ and the $g+1$ phase constants $S_k(0,0)$. Formally, letting the moduli depend on the macroscopic scales by taking $\lambda_k = \lambda_k(x,t)$ leads to a first-order system

$$\partial_t \lambda_k + c_k(\lambda_1, \ldots, \lambda_{2g+2}) \partial_x \lambda_k = 0 , \tag{5}$$

which is the generalization of the Euler system, and which (remarkably) is naturally written in a Riemann invariant form for all g. Forest and Lee showed that in the focusing problem the characteristic velocities c_k are generically complex, and thus that (5) is typically elliptic for all g, not just for $g = 0$. We shall also present evidence below that the generalized Euler system (5) is the correct model for macroscopic modulations of higher genus microstructure that spontaneously appears in the semiclassical limit of (1).

3. Current obstructions to analysis

The initial value problem (1) can of course be solved for each $\hbar$ by the inverse-scattering method [3]. The analytical challenge is to study the dependence of the solution on the small parameter $\hbar$. The solution of (1) begins with the scattering data for the nonselfadjoint Zakharov–Shabat linear system corresponding to the initial data $A(x)$ and $S(x)$,

$$\hbar\partial_x \begin{bmatrix} u_1 \\ u_2 \end{bmatrix} = \begin{bmatrix} -\mathrm{i}\lambda & A(x)\exp[\mathrm{i}S(x)/\hbar] \\ -A(x)\exp[-\mathrm{i}S(x)/\hbar] & \mathrm{i}\lambda \end{bmatrix} \begin{bmatrix} u_1 \\ u_2 \end{bmatrix} . \tag{6}$$

When $\hbar$ is small, this linear problem itself becomes semiclassical. Thus, the first step in the semiclassical analysis of the nonlinear partial differential equation (1) is the semiclassical analysis of the linear ordinary differential equation (6).

The continuous spectrum of (6) is the real λ axis. Using WKB methods to study the generalized eigenfunctions for λ real shows that the reflection coefficient is exponentially small in $\hbar$. The discrete eigenvalues can be anywhere but on the real λ axis for $\hbar$ fixed. This makes them hard to characterize generally in the limit of small $\hbar$. If $S(x) \equiv 0$, then it can be shown (an unpublished argument by Deift, Venakides, and Zhou is cited in Ref. [9]) that the eigenvalues must lie in a strip of width $\mathrm{O}(\hbar)$ around the real and imaginary axes. This single piece of information is enough to permit WKB methods to be used to find the asymptotic density of eigenvalues supported on the imaginary λ axis, where their number scales like $\hbar^{-1}$, along with asymptotic expressions for the norming constants [3,10]. If there are eigenvalues accumulating near the real λ axis, the WKB method does not find them. In the general case of nonzero $S(x)$, much less is known. Convincing numerical calculations [9] have recently suggested that the number of eigenvalues scales generally like $\hbar^{-1}$ and that the eigenvalues accumulate on contours in the plane with some asymptotic density. The contours can be quite complicated, having "y-shaped" bifurcations. At the moment, it is not at all clear how these curves are encoded in the potentials $A(x)$ and $S(x)$. However, even if one knew where the curves were, WKB methods based on real turning points cannot be used to find the asymptotic eigenvalue density and norming constants because for most λ on these curves, there are no real turning points, and the physical optics WKB solutions do not appear to break down.

If one supposes that asymptotic expressions for the eigenvalue density and norming constants are known, as they are if $S(x) \equiv 0$, then one can move on to the next step in the analysis. Because the reflection coefficient is negligible, the semiclassical solution of (1) is essentially a nonlinear superposition of a large number $N \sim \hbar^{-1}$ of solitons. In this case, the density $\rho(x,t)$ and momentum $\mu(x,t)$ (as well as all other conserved densities) can be written in terms of derivatives of a potential, $\hbar^2 \log\tau(x,t)$, where the so-called τ-function is a certain $N \times N$ determinant [3,10]. In particular, one has

$$\rho(x,t) = \partial_x^2 \hbar^2 \log\tau(x,t) , \qquad \mu(x,t) = -\partial_t\partial_x \hbar^2 \log\tau(x,t) . \tag{7}$$

In prior successful analyses that have arrived at this point (e.g., the zero-dispersion limit of the Korteweg–de Vries (KdV) equation [11], the semiclassical limit of the *defocusing* NLS hierarchy [6], and the semiclassical limit of the odd flows[3] of the focusing NLS hierarchy [10]) $\tau(x,t)$ is the determinant of a matrix $I + G(x,t)$

[3] Alas, the problem (1) is one of the even flows.

where $G(x,t)$ is Hermitean and positive definite. If $\tau(x,t)$ is then written as a sum of the principal minors of $G(x,t)$, it is evidently a sum of positive terms. It can then be shown that the largest term dominates in the limit, leading to a variational theory of the semiclassical limits of many integrable equations.

In the cases where it has been developed, the variational theory shows that different submeasures of the eigenvalue density dominate the limit for each x and t. The submeasures are generically supported on finite unions of intervals whose endpoints as functions of x and t turn out to be Riemann invariants for the hyperbolic modulation equations of microstructure made up of multiphase wavetrains (that is, they satisfy a system of the form (5) with c_k real, see Ref. [12] for KdV and Ref. [8] for NLS). The hyperbolic modulation equations for genus g multiphase wavetrains are the correct local macroscopic model until their solutions develop shocks. When this happens, the global theory shows that a region opens up within which the correct local macroscopic description is offered by the genus $g+1$ modulation equations; the microstructure becomes correspondingly more complex. In particular, for the *defocusing* version of (1), the Euler system for $\rho(x,t)$ and $\mu(x,t)$ is hyperbolic and governs the semiclassical limit until the shock time.

For the focusing problem (1), the matrix $G(x,t)$ is not Hermitean positive definite, and determining the leading contribution to $\tau(x,t)$ in the semiclassical limit remains an open problem. An analysis making use of deformations of Riemann–Hilbert matrix factorization problems is underway [13]. These deformations can be considered as a way of systematically rearranging and combining the terms in the sum for τ to reveal the dominant behavior.

4. Use of the *N*-soliton formula. Experiments

Our main purpose in this Letter is to report the results of a revealing calculation we carried out in order to better understand the semiclassical limit (1). Our approach was to avoid the analytical difficulties of the general problem, and rather to study initial data for which we could construct the solution for several small values of $\hbar$ without numerically integrating the equation.

The reflection coefficient is negligibly small. If its influence on the field $\psi(x,t)$ is ignored, then $\psi(x,t)$ can be constructed from a finite number of soliton eigenvalues and their corresponding norming constants through the solution of an algebraic linear system. If carried out on the computer, this construction is, for each fixed x and t, an independent calculation. Thus, although local errors exist (here they are exclusively due to roundoff error and its amplification through the solution of an ill-conditioned Vandermonde system), they do not accumulate from point to point and in particular do not propagate from small t to large t.

In fact, one can do better. Rather than using WKB approximations to the eigenvalues and norming constants (when they can be found), we considered the initial data

$$A(x) = A\,\mathrm{sech}(x)\,, \qquad S(x) \equiv 0\,. \tag{8}$$

Using hypergeometric functions, Satsuma and Yajima [14] solved the scattering problem exactly for this potential. With an appropriate scaling of their results, it follows that there exists a sequence $\{\hbar_N\}$ of values of $\hbar$ converging to zero,

$$\hbar_N = \frac{A}{N}\,, \qquad N = 1,2,3,\ldots\,, \tag{9}$$

for which the reflection coefficient vanishes identically and for which the eigenvalues λ_k and norming constants γ_k are known exactly. These are

$$\lambda_k = \mathrm{i}\hbar_N(k-1/2)\,, \qquad \gamma_k = (-1)^{N+k}\,, \qquad k = 1,\ldots,N\,. \tag{10}$$

For this special initial data, choosing any value of $\hbar$ in the sequence $\{\hbar_N\}$ *eliminates all errors* associated with the construction of the solution $\psi(x,t)$ except for the computational ones that arise in the construction of the

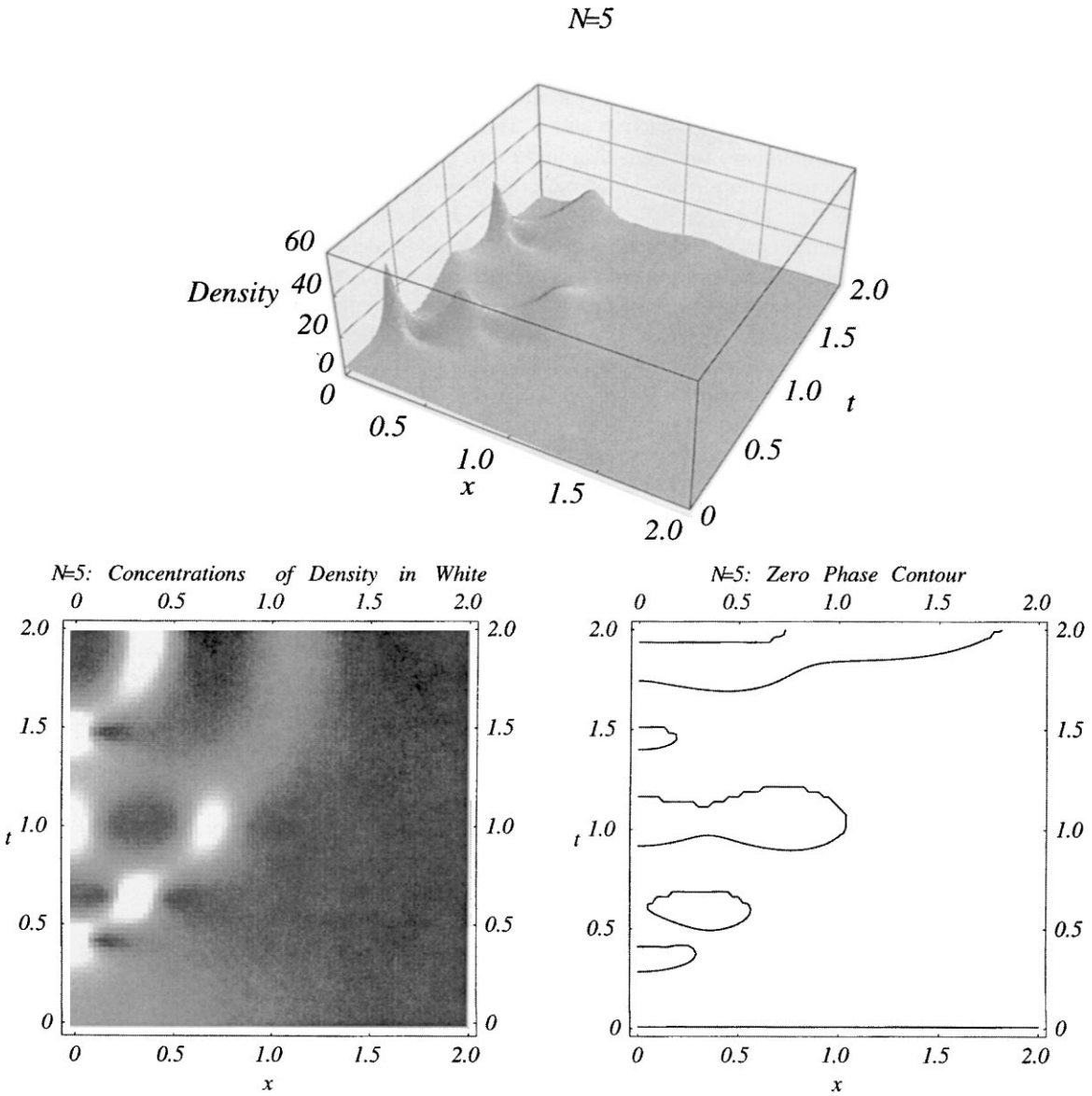

Fig. 1. $\psi(x,0) = 2\,\mathrm{sech}(x)$, $\hbar = 0.4$. Top: $\rho(x,t) = |\psi(x,t)|^2$ shown as a surface over the (x,t) plane. Bottom left: density plot of $\rho(x,t)$ in which concentrations appear in white. Bottom right: curves in the (x,t) plane where $\psi(x,t)$ is positive real.

N-soliton solution. Note that for $\hbar = \hbar_N$ fixed, the density $\rho = |\psi|^2$ is a periodic function of time t. However, the period is proportional to $\hbar^{-1}$, and thus the periodicity plays no role in our study of the behavior of the solution on space and time scales that are $O(1)$ (strictly, or smaller) in the semiclassical limit.

The $N \times N$ linear system that we chose to solve is obtained by first defining the expressions

$$F(x,t,\lambda) = \left(\lambda^N + \sum_{p=0}^{N-1} \lambda^p f_p(x,t)\right) \exp\left(-2\mathrm{i}\,\frac{\lambda x + \lambda^2 t}{\hbar}\right)$$

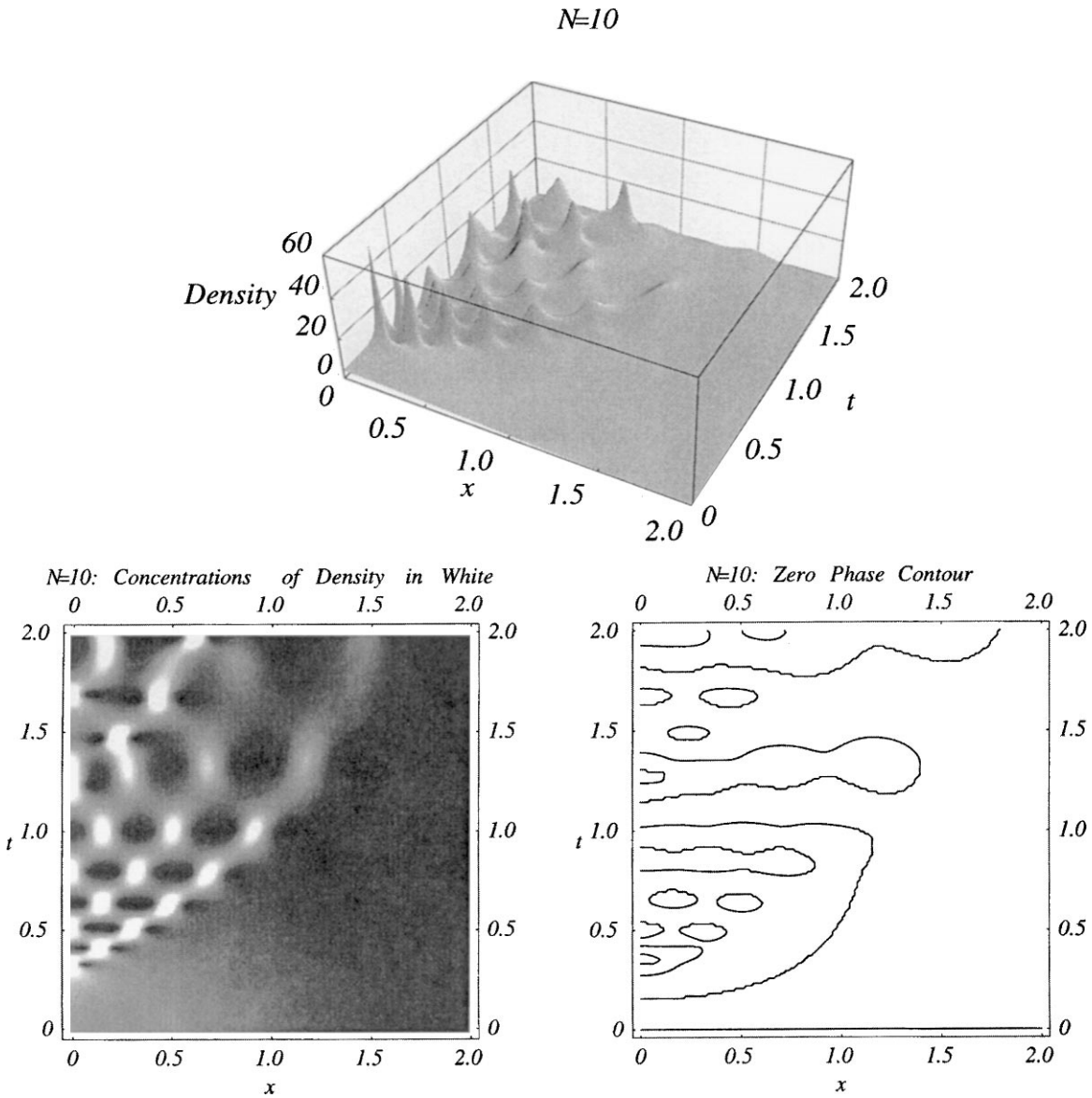

Fig. 2. $\psi(x,0) = 2\,\mathrm{sech}(x)$, $\hbar = 0.2$. See caption for Fig. 1 for clarification.

$$G(x,t,\lambda) = \sum_{p=0}^{N-1} \lambda^p g_p(x,t)\,, \tag{11}$$

where $f_0(x,t),\ldots,f_{N-1}(x,t)$ and $g_0(x,t),\ldots,g_{N-1}(x,t)$ are unknown coefficient functions. These functions are determined in terms of the data $\lambda_1,\ldots,\lambda_N$ and $\gamma_1,\ldots,\gamma_N$ by the relations

$$G(x,t,\lambda_k) = \gamma_k F(x,t,\lambda_k)\,, \qquad F(x,t,\lambda_k^*) = -\gamma_k^* G(x,t,\lambda_k^*)\,. \tag{12}$$

The $f_p(x,t)$ can be eliminated, leaving an $N \times N$ linear system for the $g_p(x,t)$. The function $\psi(x,t) =$

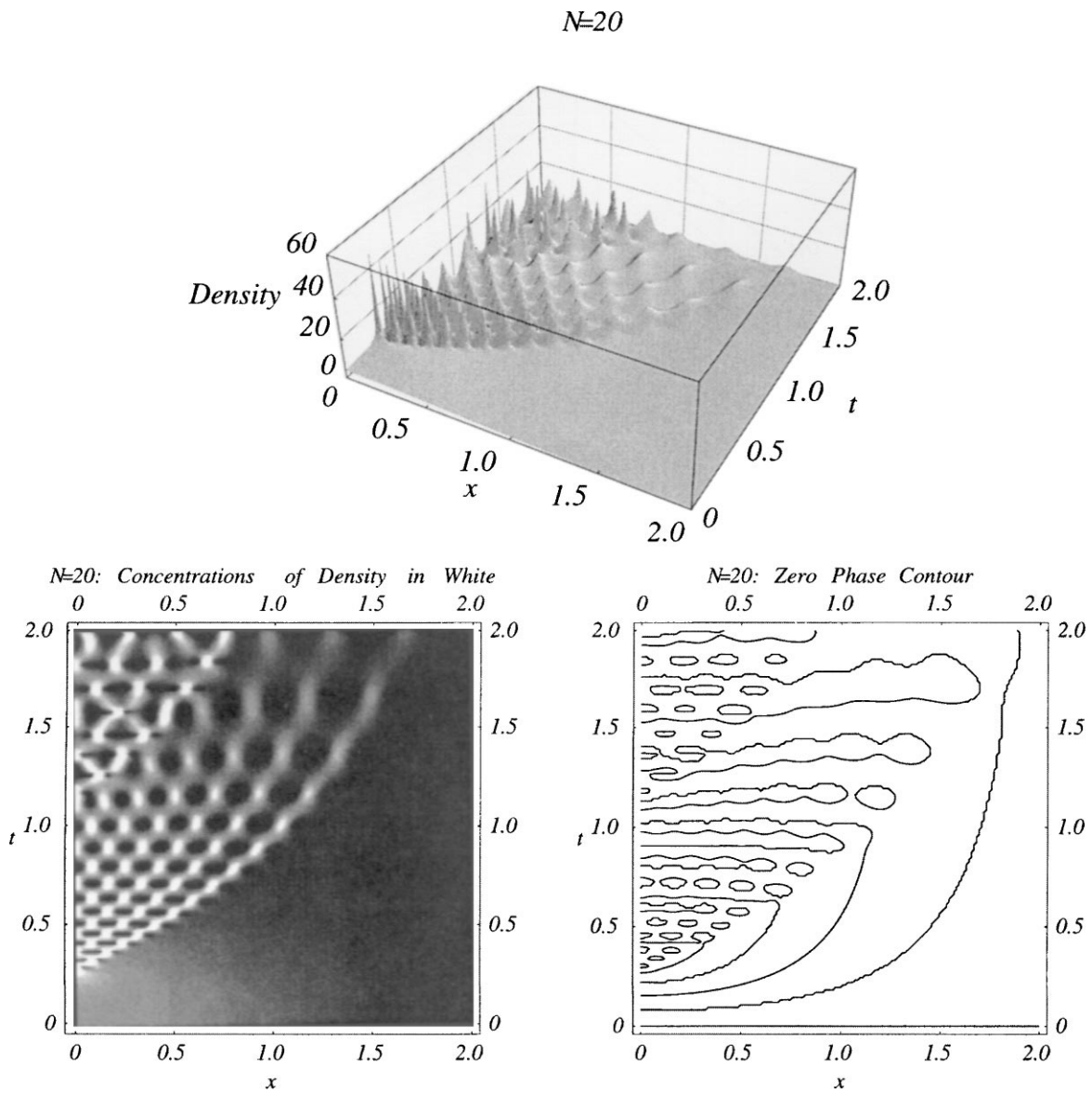

Fig. 3. $\psi(x,0) = 2\,\mathrm{sech}(x)$, $\hbar = 0.1$. See caption for Fig. 1 for clarification.

$2ig_{N-1}(x,t)$ is then a solution of (1). This algebraic procedure can be viewed as a reduction of the inverse scattering method in the case of zero reflection coefficient [3] or as an independent construction of a basis of Lax eigenfunctions from function theoretic principles (see, e.g., Ref. [15]).

We fixed $A = 2.0$ and selected the three values $\hbar_5 = 0.4$, $\hbar_{10} = 0.2$, and $\hbar_{20} = 0.1$. We then solved the linear system independently at a number of values of x and t. In our FORTRAN code it was necessary to use quadruple precision arithmetic because the linear system, although not large (only 20×20 at the largest), has a very large condition number. For the first experiment we took $N = 5$ or $\hbar = \hbar_5 = 0.4$. We constructed the solution $\psi(x,t)$ on a grid of values in the square $0 \leqslant x, t \leqslant 2$ with spacing $\Delta x = \Delta t = 0.025$. The results are shown in Fig. 1. This experiment shows the known focusing of the field due to modulational instability and

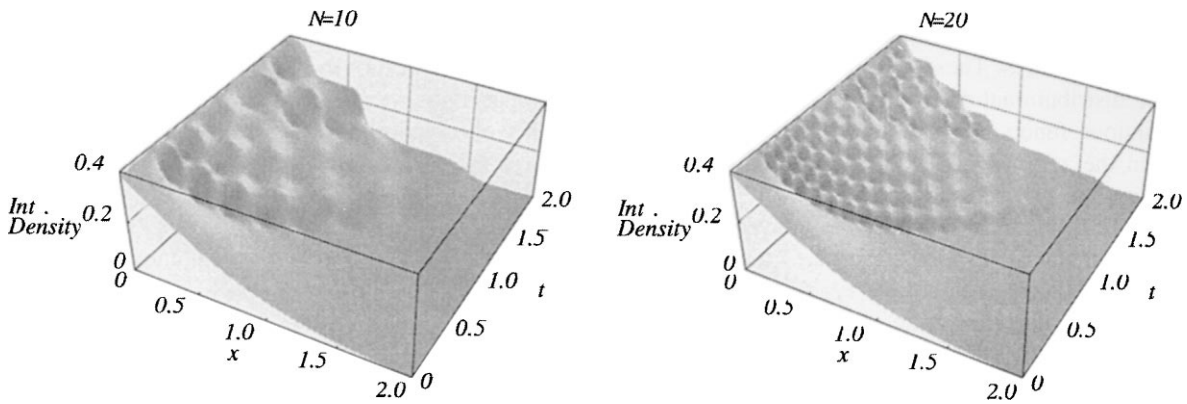

Fig. 4. Left: the density $\rho(\cdot, t)$ obtained from our experimental data for $N = 10$ or $\hbar = 0.2$, integrated in x from x to $+\infty$ for each fixed t and plotted over the (x, t) plane. Right: the same plot made for $N = 20$ or $\hbar = 0.1$. These plots suggest that the weak limit of $\rho(x, t)$ exists even beyond the primary caustic and is piecewise smooth in the (x, t) plane.

the oscillatory aftermath of the first focusing event. There is also a boundary between oscillatory and quiescent regions that one would like to interpret as the primary caustic, although at this value of $\hbar$ it is not very well resolved. To improve the resolution, we must reduce the value of $\hbar$.

The second experiment takes $\hbar$ to be half as big as in the first experiment, $\hbar = \hbar_{10} = 0.2$. The domain was again taken to be $0 \leqslant x, t \leqslant 2$, but in anticipation of more oscillatory microstructure, we sampled more often, taking $\Delta x = \Delta t = 0.0125$. The results of this experiment are shown in Fig. 2. With this refinement, the primary caustic that separates the oscillatory region from the quiescent region becomes clearly visible. Within the primary caustic, the oscillations appear to be quite regular, at least for some time during which the field is composed of a number of intermittent focus events that make up a hexagonal lattice in space-time. Such a hexagonal lattice is characteristic of multiphase wave solutions of NLS of genus $g = 2$. It can be thought of as a nonlinear interference pattern between two traveling waves (or so-called "cnoidal" waves) of genus $g = 1$; this interpretation explains the intermittency of the maxima. The width and duration of the focuses seem to scale like $\hbar$ by comparison with Fig. 1. For larger times near $x = 0$, it is difficult to conclude anything without further refinements. Also, by way of comparison with Fig. 1, it appears that the phase gradient scales like $\hbar^{-1}$, at least outside the primary caustic. This, along with the behavior of ρ in this region begins to suggest strong convergence of $\rho(x, t)$ and $\mu(x, t)$ outside the primary caustic.

The third experiment again divides $\hbar$ in half, giving $\hbar = \hbar_{20} = 0.1$, the same value as was used in the numerical experiment reported in Ref. [5]. The domain and sampling are the same as in the second experiment. The results are shown in Fig. 3. This experiment, again taken in comparison with the two prior ones, shows very clearly both the primary caustic and the hexagonal lattice of focuses characteristic of modulated genus two waves. Furthermore, it is now clear that for larger t, a *secondary caustic* appears that separates the modulated genus two waves from a field of more complicated (although evidently still regular) microstructure. This has never been seen before. The phase contours give yet more evidence for the strong convergence of $\rho(x, t)$ and $\mu(x, t)$ outside the primary caustic.

We have integrated the data for $\rho(x, t)$ with respect to x in an effort to study the weak convergence of $\rho(x, t)$ beyond the primary caustic. With the definition

$$R(x, t) \doteq \int_x^\infty \rho(z, t)\, \mathrm{d}z\,, \tag{13}$$

we show in Fig. 4 plots of $R(x, t)$ calculated from our numerical data for $N = 10$ (or $\hbar = 0.2$) and $N = 20$

(or $\hbar = 0.1$). These plots suggest that as $\hbar$ goes to zero, $R(x,t)$ converges strongly to a continuous function $R_0(x,t)$ that is piecewise smooth. The limit function appears to have discontinuities in the first x derivative at the caustic curves. These qualities of the strong limit $R_0(x,t)$ suggest in turn the weak convergence of $\rho(x,t)$ to the distributional derivative $\rho_0(x,t) \doteq -\partial_x R_0(x,t)$. The weak limit $\rho_0(x,t)$ then appears to be a piecewise continuous function, with discontinuities at the caustics. This observation agrees with what is known to be true in the zero-dispersion limit of the KdV equation [11] and the semiclassical limit of the defocusing NLS equation [6].

Before the primary caustic, the convergence of $\rho(x,t)$ appears to be strong, as is that of the momentum $\mu(x,t)$. In fact, we have constructed the quantities $\rho(x,t)$ and $\mu(x,t)$ from our data for the complex field $\psi(x,t)$ and have been able to verify their strong convergence outside the primary caustic. Moreover, we have checked that these quantities are approximate solutions of the *elliptic* Euler system (that is, of (3) with $\hbar$ set equal to zero). Although the initial value problem for the Euler system is ill-posed, it can be solved uniquely for (at least) analytic initial data by Cauchy–Kovaleskaya series. A contour plot of the first twenty terms of the series expansions for $\rho(x,t)$ and $\mu(x,t)$ about $t = 0$ are compared with $\rho(x,t)$ and $\mu(x,t)$ as calculated from our data for $N = 20$, or $\hbar = 0.1$, in Fig. 5. In the series pictures, the curve where the contours accumulate may be identified as $t = R(x)$, the radius of convergence of the series in t as a function of x. For $t < R(x)$ we observe good agreement between the series solution and our data for $\hbar = 0.1$. The radius of convergence $t = R(x)$ is evidently *not* the same as the primary caustic. However, this radius only appears to be an obstruction to analytic continuation at the first focus which occurs at $x = 0$. For other values of x, we have noted that the sequence of partial sums of the Cauchy–Kovalevskaya series diverges beyond the radius in an oscillatory manner, suggesting a singularity for complex t and the possibility of analytic continuation in real t beyond the radius. For each x, there is some real time $t = t_1(x)$ beyond which the series solution cannot be analytically continued; we believe *this* to be the primary caustic.

Within the radius of convergence, it is possible to be more precise about the error. For each fixed t before the first focus, we evaluated the L_∞ norm in x of the difference between $\rho(x,t)$ as computed from our numerical data and $\rho(x,t)$ as calculated from the twenty-term Cauchy–Kovalevskaya series approximant. We further divided this norm by $\hbar^2$ and plotted the resulting scaled norm as a function of t for $N = 10$ (or $\hbar = 0.2$) and $N = 20$ (or $\hbar = 0.1$). The results are shown in Fig. 6. The graphs for $N = 10$ and $N = 20$ are almost indistinguishable to the eye. This is strong evidence that the error in approximating the semiclassical solution of NLS before the primary caustic by the solution of the elliptic Euler system is $O(\hbar^2)$. Note that it is not at all clear from the graphs whether this error is uniformly small as t approaches the time of the first focus.

At the primary caustic, the microstructure appears to change from genus $g = 0$ to genus $g = 2$; this kind of phase transition should be compared with those occurring in the semiclassical theory of KdV and defocusing NLS where the genus typically increases by one at the caustic[4]. From the three experiments, it is possible to observe that while the number of focuses in any fixed region of x and t between the primary and secondary caustics scales like $\hbar^{-1}$, their amplitude converges to a smooth function of x and t. Our experiments are not detailed enough at this time to tell whether this smooth amplitude function becomes unbounded in the neighborhood of the first focus. However, this observation suggests that the moduli of the genus two microstructure are, in the limit, well-defined smooth functions of x and t in this region. We thus anticipate that the modulations of the waves in this region between the primary and secondary caustics are governed by the $g = 2$ elliptic modulation equations (5) of Forest and Lee [8]. A global theory, once developed, will give the matching conditions across the primary caustic, beyond which the $g = 2$ elliptic system presumably gives

[4] The difference between the two kinds of phase transition can be explained by the fact that the moduli λ_k come in non-real complex conjugate pairs for focusing NLS and must be real in the KdV and defocusing NLS cases. The onset of a phase transition is indicated by the unfolding of a double point of the Riemann surface. While for the real spectrum problems it is possible for an isolated double point to appear anywhere on the real axis and split, increasing the genus by one, in the focusing NLS case the generic situation is for a pair of complex conjugate non-real double points to open up, thus creating two new "handles" and increasing the genus by two.

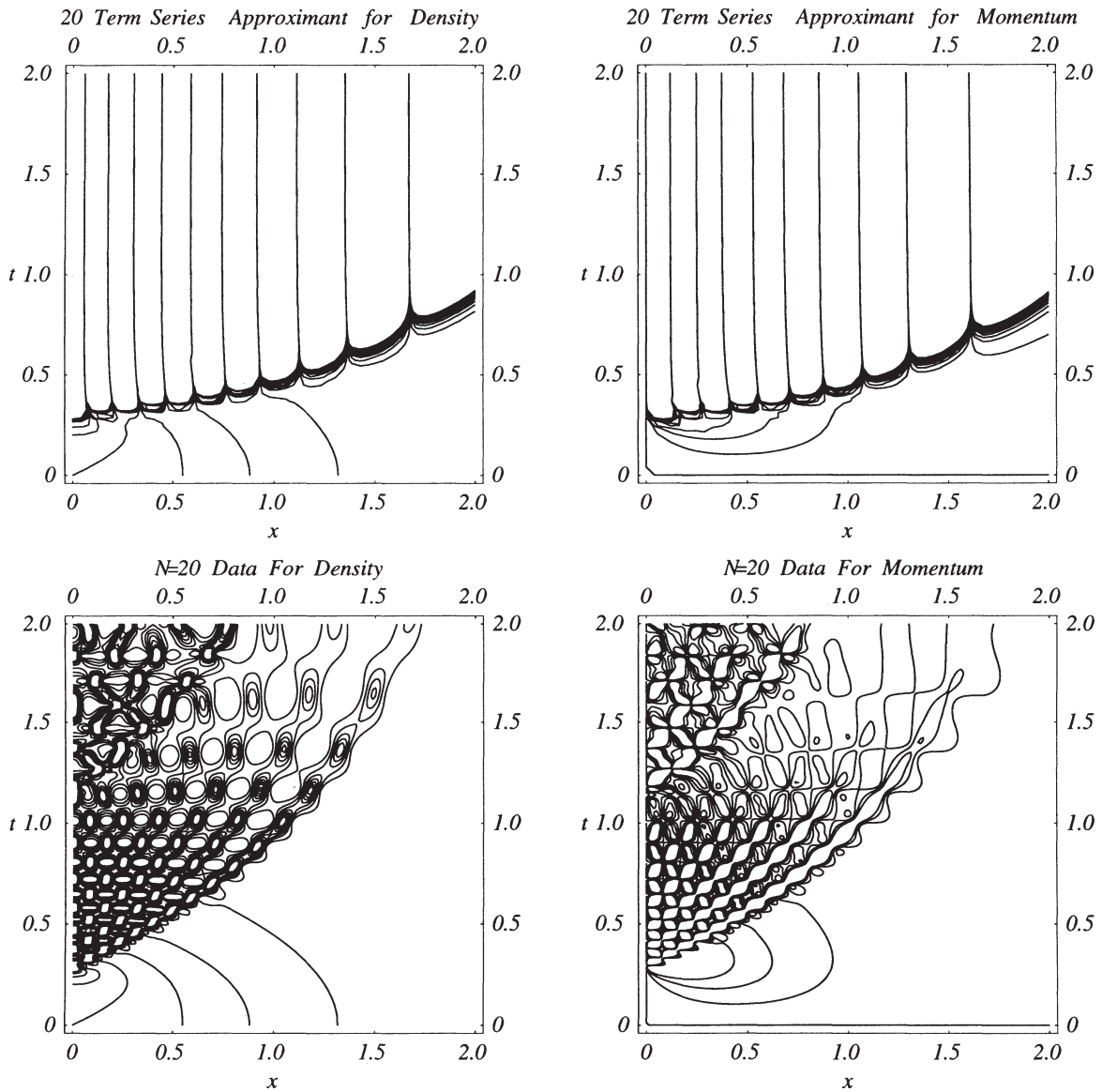

Fig. 5. Upper left (right): contour plot of the first twenty terms of the series solution for $\rho(x,t)$ ($\mu(x,t)$) about $t = 0$. Lower left (right): contour plot of $\rho(x,t)$ ($\mu(x,t)$) as calculated from our experimental data for $N = 20$ or $\hbar = 0.1$.

the behavior until the time $t = t_2(x)$ at which the solution ceases to be analytic at the secondary caustic. We expect the process to continue indefinitely, with a cascade of increasingly complicated microstructure governed by elliptic modulation equations and separated by a sequence of caustic curves at which the solutions to the elliptic equations lose analyticity. Our experiments do not address the way in which the solutions to the elliptic equations become singular, whether through the formation of poles, branch points, or more exotic natural boundaries. This is clearly a topic for further study.

The qualitative agreement of our calculations using the N-soliton solution with numerical experiments carried out for more general initial data suggest that our observations should apply to arbitrary analytic initial data.

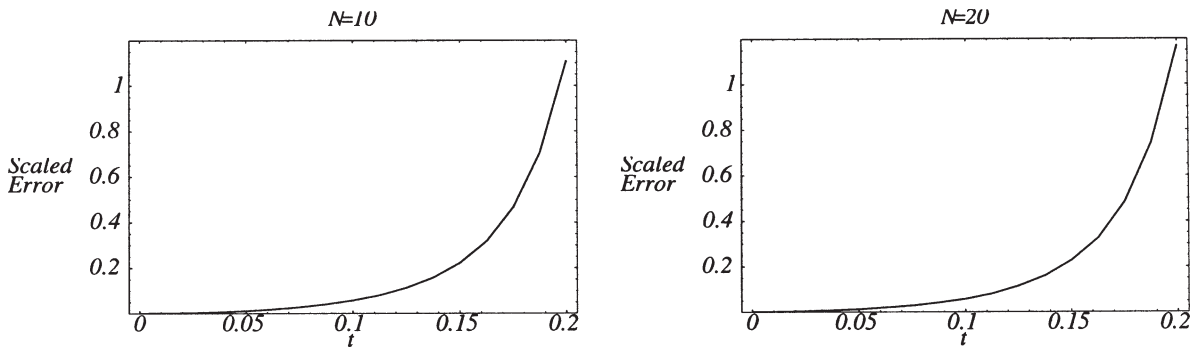

Fig. 6. Left: the L_∞ norm, divided by $\hbar^2$, of the difference between $\rho(\cdot,t)$ as computed from the first twenty terms of the Cauchy–Kovalevskaya series and $\rho(\cdot,t)$ as calculated from our experimental data for $N = 10$ or $\hbar = 0.2$. Right: the same comparison made with our experimental data for $N = 20$ or $\hbar = 0.1$. These plots show that the error is order $O(\hbar^2)$, although not necessarily uniformly as t approaches the first focus.

So what happens for nonanalytic initial data? Although the Cauchy–Kovalevskaya procedure fails in this case, the existence of solutions of the initial value problem for the elliptic Euler system and its generalization (5) is not ruled out. In the analogous problem of vortex sheet motion, solutions to the ill-posed initial value problem can indeed be found for initial data with singularities in some derivatives [7]. However, we do expect the ill-posedness of the initial value problem for the Euler system to appear as a certain sensitive dependence of the solution on initial data that should be understood. We hope that we have convinced some readers that the elliptic modulation equations (5) for NLS [8] deserve further study.

Acknowledgement

We would like to thank D.W. McLaughlin, K.T.-R. McLaughlin, P. Deift, and R. Krasny for useful discussions.

References

[1] M.G. Forest, K.T.-R. McLaughlin, J. Nonlinear Sci. 7 (1998) 43.
[2] V.L. Ginzburg, L.P. Pitaevskii, Sov. Phys. JETP 34 (1958) 858 [Z. Eksp. Teor. Fiz. 34 (1958) 1240].
[3] V.E. Zakharov, A.B. Shabat, Sov. Phys. JETP 34 (1972) 62 [Z. Eksp. Teor. Fiz. 61 (1971) 118].
[4] J.C. Bronski, D.W. McLaughlin, Semiclassical behavior in the NLS equation: optical shocks – focusing instabilities, in: Singular Limits of Dispersive Waves, NATO ASI Series, Vol. 320, N.M. Ercolani et al., eds. (Plenum, New York, 1994).
[5] S. Jin, C.D. Levermore, D.W. McLaughlin, The behavior of solutions of the NLS equation in the semiclassical limit, in: Singular Limits of Dispersive Waves, NATO ASI Series, Vol. 320, N.M. Ercolani et al., eds. (Plenum, New York, 1994).
[6] S. Jin, C.D. Levermore, D.W. McLaughlin, The semiclassical limit of the defocusing NLS hierarchy, Commun. Pure Appl. Math. (1997), submitted.
[7] R.E. Caflisch, O.F. Orellana, SIAM J. Math. Anal. 20 (1989) 293.
[8] M.G. Forest, J-.E. Lee, Geometry and modulation theory for the periodic nonlinear Schrödinger equation, in: Oscillation Theory, Computation, and Methods of Compensated Compactness, IMA, Vol. 2, C. Dafermos et al., eds. (Springer, New York, 1986).
[9] J.C. Bronski, Physica D 97 (1996) 376.
[10] N.M. Ercolani, S. Jin, C.D. Levermore, W. MacEvoy Jr., The zero dispersion limit of the NLS/mKdV hierarchy for the nonselfadjoint ZS operator (1993), preprint.
[11] P.D. Lax, C.D. Levermore, Comm. Pure Appl. Math. 36 (1983) 253, 571, 809.
[12] H. Flaschka, M.G. Forest, D.W. McLaughlin, Comm. Pure Appl. Math. 33 (1980) 739.
[13] S. Kamvissis, K.T.-R. McLaughlin, P.D. Miller, in preparation.
[14] J. Satsuma, N. Yajima, Suppl. Prog. Theor. Phys. 55 (1974) 284.
[15] P.D. Miller, N.N. Akhmediev, Phys. Rev. E 53 (1996) 4098.